Turk J Chem
33 (2009) , 589 – 598.

doi:10.3906/kim-0809-34

Kinetics of CO oxidation over Pt-CeO_x supported on air-oxidized activated carbon

Berrin GÜLYÜZ, Şeyma ÖZKARA AYDINOĞLU, Ahmet Erhan AKSOYLU, Zeynep İlsen ÖNSAN*
Department of Chemical Engineering, Boğaziçi University, Bebek 34342, İstanbul-TURKEY
e-mail: onsan@boun.edu.tr

Received 08.09.2008

Kinetics of low-temperature CO oxidation was studied under atmospheric pressure at 383 K in the initial rates region over 1wt%Pt-1wt%CeO_x supported on air-oxidized activated carbon (AC2). Feed concentrations of 1-5 mol% CO and 1-2.5 mol% O_2 with balance He were used for CO oxidation in the absence of hydrogen. A simple power-function rate expression was obtained with reaction orders of -0.24 in CO and 0.98 in O_2, and a plausible LHHW expression compatible with mechanisms reported in the literature was proposed. Feed concentrations of 5 mol% CO and 2.5 mol% O_2 were used for investigating the effect of the presence of CO_2 or H_2 on CO oxidation rates by partially replacing inert He with 2-4 mol% CO_2 or 10-60 mol% H_2.

Key Words: Carbon monoxide, oxidation, kinetics, Pt-ceria catalysts, activated carbon supports, PROX.

Introduction

A major constraint in the operation of proton-exchange membrane (PEM) fuel cells is the necessity to supply CO-free hydrogen, which means that the 0.5-1 mol% CO present in the effluent from the low-temperature water-gas shift converter of a fuel processor must be reduced to 10-50 ppm before the hydrogen stream enters the PEM fuel cell. Selective low-temperature CO oxidation is an effective route for final CO removal at 373-423 K.[1−3] Supported noble metal catalysts that are normally considered for promoting CO oxidation are not efficient at low O_2/CO ratios and/or temperatures below 443 K for the reason that CO and O_2 adsorb on similar sites, and O_2 adsorption is hindered by strong CO adsorption.[4] Noble metal reducible oxide (NMRO) catalysts display much higher catalytic activity as they offer suitable sites for both CO and O_2 adsorption; numerous promoted precious metal catalysts were considered for this purpose.[1,2]

*Corresponding author

The importance of a reducible component such as CeO_2 becomes evident when the performances of Pt catalysts with and without CeO_2 are compared. CeO_2 is reported to sustain CO oxidation by enhancing the O_2 supply to Pt sites.[5] For instance, the addition of CeO_2 to Pt/γ-Al_2O_3 decreases both the reaction order in O_2 and the apparent E_A for CO oxidation,[6] and Pt/CeO_2 performs better than Pt/γ-Al_2O_3 in terms of CO oxidation.[7] The surface states of Pt/CeO_2 during CO oxidation in the presence of H_2 were explored by spectroscopic techniques, which clearly showed CO adsorption on Pt sites and the existence of considerable water on the CeO_2 surface.[8] It was suggested that oxygen-deficient CeO_2 stabilizes the surface water, which inhibits H_2 oxidation and reacts at the metal-support interface with adsorbed CO in a water-gas shift or WGS-type reaction to produce CO_2.[9] CO oxidation mechanisms on Pt/CeO_2 and Pd/CeO_2 were studied by in situ experimental methods, which indicated that while Pt/CeO_2 is an exceptional PROX catalyst Pd/CeO_2 is not because of its affinity for hydrogen chemisorption.[10]

PROX performances of several co-impregnated and sequentially impregnated Pt-CeO_x catalysts supported on non-oxidized, air-oxidized, and HNO_3-oxidized activated carbons (AC1, AC2, and AC3, respectively) were studied in experiments conducted at atmospheric pressure and 423 K in the absence[11] and presence[12] of CO_2 and H_2O in the feed. Although the CO conversions obtained with a molar feed composition of 1% CO, 1% O_2, and 60% H_2 with 38% inert He as balance remained in the range of 20%, the addition of 15% CO_2 and 10% H_2O into the feed by partially replacing the inert He proved sequentially impregnated 1wt%Pt-1wt%CeO_x/AC2 to be the best catalyst, giving 100% CO conversion with 50% selectivity for CO oxidation at all times-on-stream. These results are in agreement with reports on the role of surface water in (a) increasing the WGS effect, (b) reducing the activation energy of CO oxidation, and (c) forming hydroxyl groups that may also participate in the oxidation of CO and H_2.[2,9]

The motivation of the present work was to assess the low-temperature CO oxidation performance of 1wt%Pt-1wt%CeO_x/AC2 in the absence of H_2 to find the CO and O_2 dependence of CO oxidation rates, to suggest a plausible Langmuir-Hinshelwood-Hougen-Watson expression compatible with the data, and then to examine the effects of the presence of CO_2 or H_2 in the feed on CO removal rates.

Experimental

Catalyst preparation

Commercial activated carbon NORIT ROX, crushed and sieved to 255-344 microns, was treated with 2N HCl to get rid of its ash and sulfur content, washed thoroughly with water to remove the HCl, and further oxidized at 723 K for 10 h under a nitrogen-dry air mixture (75:25 by volume) to develop its textural and surface chemical properties. The properties of various AC supports and the detailed procedures for AC support preparation have previously been reported in detail;[13,14] air-oxidized AC2 has a BET surface area of 1273 $m^2\ g^{-1}$, mesopore surface area of 195 $m^2\ g^{-1}$, and micropore volume of 0.47 $cm^3\ g^{-1}$. Bimetallic 1wt%Pt-1wt%CeO_x/AC2 was prepared by sequential incipient-to-wetness impregnation of $Ce(NO_3)_3.6H_2O$ and $H_2PtCl_6.6H_2O$ solutions, respectively, followed by drying overnight at 388 K, as described earlier,[11,12] with the exception that an intermediate heat treatment at 673 K under He was not performed between 2 impregnations. Prior to each reaction experiment, the catalyst sample was heat treated in situ for 2 h at 673 K under He flow and then reduced at the same temperature for 2 h under H_2 flow.

Reaction experiments

Reaction experiments were conducted using 4-mm i.d. stainless steel tubular down-flow micro-reactors placed in the constant-temperature zone of a 2.4-cm i.d. × 50 cm tube furnace controlled to ±0.1 K by a Shimaden FP-21 programmable controller. The flow rates of research grade CO, CO_2, H_2, inert He gases, and O_2/He mixtures were controlled by calibrated Brooks 5850E and Aalborg GFC mass flow controllers. Reactant and product streams were analyzed using an ATI UNICAM 610 Series temperature-controlled and programmable gas chromatograph equipped with a TCD and a concentric column (CTR I) operated at 303 K under 35 cm^3 min^{-1} He carrier.

CO oxidation was studied under atmospheric pressure at a temperature of 383 K using 100-250 mg of fresh catalyst particles and total feed flow rates between 100 and 150 cm^3 min^{-1}. Silane-treated glass wool (Alltech) was used to fix the position of the catalyst bed. Preliminary experiments conducted under reaction conditions showed that (a) the stainless steel reactor and glass wool were inert, (b) 250-344 μm catalyst particles were sufficiently small for neglecting internal diffusion effects, and (c) external mass transfer effects were insignificant within the gas flow rate ranges selected.

Feed concentrations of 1-5 mol% CO and 1-2.5 mol% O_2 with balance He were used for studying CO oxidation kinetics in the absence of hydrogen. Feed concentrations of 5 mol% CO and 2.5 mol% O_2 were used to investigate the effects of the presence of CO_2 and H_2 on CO oxidation rates by partially replacing the inert helium with 2-4 mol% CO_2 or 10-60 mol% H_2.

CO and O_2 conversions and the process parameter for describing oxygen excess, λ, were defined by the following equations:[15]

$$X_{CO}(\%) = \frac{[CO]_{in} - [CO]_{out}}{[CO]_{in}} \times 100 \tag{1}$$

$$X_{O_2}(\%) = \frac{[O_2]_{in} - [O_2]_{out}}{[O_2]_{in}} \times 100 \tag{2}$$

$$\lambda = \frac{2C_{O_2}}{C_{CO}} = \frac{2P_{O_2}}{P_{CO}} \tag{3}$$

CO oxidation experiments were performed under differential conditions to collect intrinsic kinetic data in the initial rates range. The reaction rates, ($-R_{CO}$), were calculated from conversion versus space time ($W_{cat}/F_{CO_{in}}$) data:

$$(-R_{co}) = \frac{x_{CO}}{W/F_{CO_{in}}} \tag{4}$$

where x_{CO} symbolizes CO conversion, $F_{CO_{in}}$ is inlet CO flow rate in μmol s^{-1}, W_{cat} is the catalyst weight in mg, and ($-R_{CO}$) is the reaction rate in μmol g^{-1} s^{-1}. The space time (g s μmol^{-1}) is defined as the ratio of mass of catalyst (W_{cat}) to the molar flow rate of CO at the reactor inlet, F_{CO}. CO conversions were kept well below 10% in kinetic measurements performed under differential conditions, and data obtained at 90 min time-on-stream (TOS) were used in the calculation of reaction rates.

Results and discussion

Kinetics of CO oxidation over 1wt%Pt-1wt%CeO_x/AC2

Low-temperature CO oxidation on the 1wt%Pt-1wt%CeO_x/AC2 catalyst was initially studied in the absence of H_2. A temperature of 383 K was selected for intrinsic kinetic analysis conducted in the initial rates region using CO concentrations between 1 and 5 mol% at various O_2/CO molar ratios (λ = 0.67-2.0) and space times (W/F_{CO} = 0.04-0.22 g s μmol^{-1}). O_2/CO ratio is a key factor in determining the state of the catalyst surface, i.e. the reducibility of CeO_x as well as the process of surface transfer of oxygen from CeO_x to Pt sites involving interaction between mobile oxygen and oxygen-bearing surface groups and/or low coordination carbon atoms present on the AC2 surface; both phenomena influence the reaction mechanism and kinetics. Excess CO in the feed decreases catalytic activity by blocking Pt sites, becoming significant when the rate of oxygen reverse spillover to Pt sites is lower than the rate of CO adsorption on these sites. In this work, λ values between 0.67 and 2.0 were included in the analysis in order to account for O_2/CO ratios lower and higher than the stoichiometric.

CO conversion (X_{CO}) data taken at constant feed composition and different space times were used to verify linear behavior in the initial rates region. Five different CO concentrations and 4 different O_2 concentrations corresponding to 4 different O_2/CO ratios were used, and experimental runs were conducted at 1-3 different space times for each feed composition. Initial rates of CO conversion were extracted from intrinsic kinetic data taken at 383 K in 17 duplicate experiments under conditions where maximum CO conversions were less than 10%. The initial rates used in the kinetic analysis are given in Table 1. Oxygen conversions (X_{O_2}) were also measured in all runs largely for data control reasons. Examples of X_{CO} and X_{O_2} values measured at different feed compositions are given in Table 2 to show the CO conversion and space time ranges used in the kinetic analysis of CO consumption.

Table 1. Initial rates of low-temperature CO oxidation at 383 K over 1wt%Pt-1wt%CeO_x/AC2 (W/F_{CO} = 0.04-0.22 g s μmol^{-1}; TOS = 90 min).

P_{CO} (atm)	P_{O_2} (atm)	λ	Number runs*	(-R_{CO}) (μmol s^{-1} g^{-1})	R^2
0.01	0.01	2	3	0.3972	0.985
0.02	0.01	1	4	0.3038	0.925
0.03	0.01	0.67	2	0.3276	0.998
0.03	0.015	1	3	0.4359	0.940
0.04	0.02	1	1	0.5452	-
0.05	0.02	0.80	2	0.5080	0.988
0.05	0.025	1	2	0.6569	0.999

*Number of duplicated experiments conducted at different space times.

Table 2. CO and O_2 conversions at different feed compositions and space times (1wt%Pt-1wt%CeO_x/AC2; T = 383 K; TOS = 90 min).

P_{CO} (atm)	P_{O_2} (atm)	λ	W/F_{CO} (g s μmol^{-1})	X_{CO}	X_{O_2}
0.01	0.01	2	0.220	0.091	0.033
0.02	0.01	1	0.049	0.028	0.022
0.03	0.01	0.67	0.098	0.034	0.060
0.03	0.015	1	0.122	0.058	0.060
0.04	0.02	1	0.073	0.040	0.046
0.05	0.02	0.80	0.059	0.035	0.039
0.05	0.025	1	0.039	0.026	0.026

The power-function rate expression for CO conversion was proposed as follows:

$$(-R_{CO}) = k\,(P_{CO})^{\alpha}\,(P_{O_2})^{\beta} \tag{5}$$

The reaction orders (α and β) and the apparent rate constant (k) were estimated by non-linear regression analysis minimizing the sum of the squared differences of calculated and experimental CO oxidation rates using the Levenberg-Marquardt algorithm in POLYMATH 5.1 environment. Reaction orders in CO and O_2 were determined as -0.24 and 0.98, respectively, indicating that the rate of CO oxidation is directly proportional to the O_2 partial pressure but is hampered by the CO partial pressure to some extent. The apparent reaction rate constant (k) was estimated as 11.5 μmol g^{-1} s^{-1} atm$^{-0.74}$. The following power rate law was obtained for low-temperature CO oxidation over the 1wt%Pt-1wt%CeO_x/AC2 catalyst at 383 K:

$$(-R_{CO}) = 11.5\,(P_{CO})^{-0.24}\,(P_{O_2})^{0.98}\,\mu molg^{-1}s^{-1} \tag{6}$$

The variance σ^2 of experimental CO consumption rates and those predicted by Eq. (6) was determined as 0.00047 (μmol g^{-1} s^{-1})^2. The fit between calculated and experimentally measured rates is shown in Figure 1.

One of the reaction regimes frequently encountered in CO oxidation over supported Pt catalysts at relatively low temperatures and/or lower λ values involves almost complete coverage of the catalyst surface by adsorbed CO, which effectively impedes O_2 adsorption, thus leading to negative reaction orders close to unity for CO and positive reaction orders close to unity for O_2.[16] This reaction regime is called the "low-rate branch", because the negative CO dependence means a surface saturated by CO, which permits low surface concentrations of O_2 only and causes dissociative oxygen adsorption to limit the reaction rate.[17] The reaction orders obtained in the present kinetic analysis with respect to CO (-0.24) and O_2 (0.98) indicate that CO oxidation is occurring in the "low-rate branch". The fact that the negative order of CO is much lower than unity can be attributed to (a) the contribution of the reducible component, CeO_x, that promotes CO oxidation by increasing the oxygen supply to Pt sites,[5] and (b) the involvement of oxygen-bearing surface groups of the air-oxidized support, AC2, in the stabilization and rapid transport of oxygen atoms from CeO_x to Pt sites. In addition, the oxygen-bearing surface groups on the AC2 support may also decompose and leave low-coordination carbon atoms which may accept oxygen and transfer it to metal/metal oxide sites.[13] As a result of these effects,

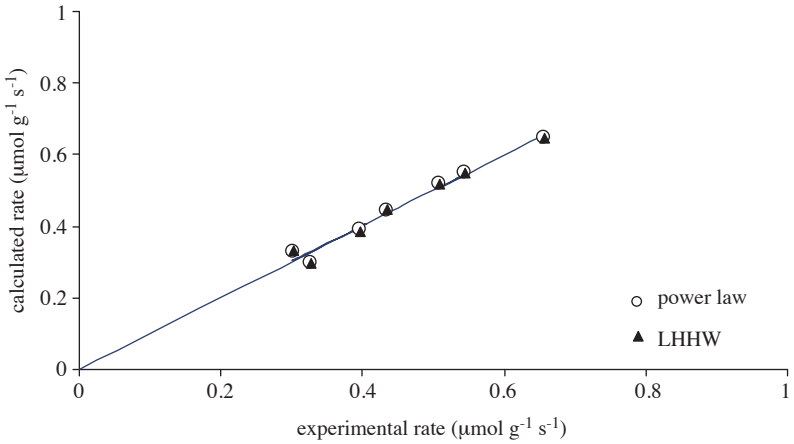

Figure 1. Experimental versus calculated rates of low-temperature CO oxidation at 383 K over 1wt%Pt-1wt%CeO_x/AC2.

the surface reaction may be assumed to happen between CO and oxygen adsorbed in proximity on Pt sites or at their peripheries.[15] A synergistic interaction brought about by fast oxygen reverse spillover from CeO_x sites on to Pt sites can also increase CO oxidation rates.[6]

CO consumption rates extracted from intrinsic kinetic data (Table 1) were also used for testing Langmuir-Hinshelwood-Hougen-Watson rate models based on mechanisms proposed in the literature.[16–18] In view of the negative reaction order of CO in the power function rate expression (Eq. (6)), molecular adsorption of CO on Pt sites may be assumed to be the fastest step in the reaction mechanism, accompanied by relatively slow dissociative oxygen adsorption on the CeO_x surface. Subsequent oxygen reverse spillover from CeO_x to Pt sites is likely to be facilitated by the oxygen-bearing surface groups of AC2 in the case of 1wt%Pt-1wt%CeO_x/AC2. Molecular bridge-type CO adsorption on Pt sites is reported to start after ca. 25% surface coverage and become increasingly favored at higher coverages;[19] this has also been confirmed by scanning tunnel microscopy.[20] One of the most plausible mechanisms was found to be CO oxidation on Pt sites or at the Pt-CeOx interface between neighboring CO and oxygen species, with dissociative adsorption of oxygen on CeO_x as the rate-limiting step. The LHHW equation obtained by recognizing the abundance of reactive bridge-bonded CO species and neglecting the surface concentration of oxygen in the adsorption term is as follows:

$$(-R_{CO})_o = \frac{kP_{o_2}}{(1 + K_{co}P_{co})^{1/2}} \tag{7}$$

Non-linear regression in the POLYMATH 5.1 environment was used for model discrimination and parameter estimation. The optimum values of the rate parameters were estimated to be $k = 64.5\ \mu\text{mol g}^{-1}\ \text{s}^{-1}\ \text{atm}^{-1}$ and $K_{CO} = 45.0\ \text{atm}^{-1}$. The variance σ^2 of experimental CO oxidation rates and those calculated by Eq. (6) was determined as 0.00042 $(\mu\text{mol g}^{-1}\ \text{s}^{-1})^2$. Experimentally measured CO oxidation rates are compared with model-predicted rates in Figure 1 using power law and LHHW rate expressions, both of which are in good agreement.

The power function rate expression obtained simply by data fitting is compatible with a plausible LHHW model derived from a justifiable reaction mechanism involving bridge-bonding of CO on Pt sites, slow dissociative

adsorption of oxygen on CeO_x followed by oxygen reverse spillover from CeO_x to Pt sites, and a surface reaction between adjacent CO and oxygen species on Pt or at the Pt-CeO_x interface. The LHHW model of Eq. (6) can be reduced approximately to the power law expression of Eq. (6) by assuming that $(K_{CO}P_{CO})^{1/2} >> 1$.

Effect of CO_2 on CO oxidation

The influence of CO_2 on CO conversions and CO oxidation rates was studied in the initial rates region at 383 K, by partly replacing the inert He with 2-4 mol% CO_2 in a feed containing 5 mol% CO and 2.5 mol% O_2. The CO conversions and CO oxidation rates obtained at a space time of 0.049 g s μmol^{-1} and λ value of 1.0 are given in Table 3. These data show that the CO conversion decreases slowly at first with the addition of 2-3 mol% CO_2, but a fast decline ensues at CO_2 concentrations above 3.5 mol%, leading to a similar decrease in CO oxidation rates.

Table 3. Effect of H_2 and CO_2 on CO conversions and CO oxidation rates (T = 383 K; W/F_{CO} = 0.049 g s μmol^{-1}; λ = 1.0; TOS = 90 min).

CO atm	O_2 atm	H_2 atm	CO_2 atm	X_{CO}	$(-R_{CO})$ (μmol s^{-1} g^{-1})
0.05	0.025	-	-	0.033	0.674
0.05	0.025	0.10	-	0.032	0.653
0.05	0.025	0.15	-	0.029	0.592
0.05	0.025	0.20	-	0.025	0.510
0.05	0.025	0.40	-	0.021	0.429
0.05	0.025	0.60	-	0.020	0.408
0.05	0.025	-	0.020	0.039	0.796
0.05	0.025	-	0.025	0.034	0.694
0.05	0.025	-	0.030	0.031	0.633
0.05	0.025	-	0.035	0.019	0.388
0.05	0.025	-	0.040	0.011	0.225

The influence of CO_2 on CO conversions and CO oxidation rates was studied in the initial rates region at 383 K, by partly replacing the inert He with 2-4 mol% CO_2 in a feed containing 5 mol% CO and 2.5 mol% O_2. The CO conversions and CO oxidation rates obtained at a space time of 0.049 g s μmol^{-1} and λ value of 1.0 are given in Table 3. These data show that the CO conversion decreases slowly at first with the addition of 2-3 mol% CO_2, but a fast decline ensues at CO_2 concentrations above 3.5 mol%, leading to a similar decrease in CO oxidation rates.

There are 2 fairly distinct regions in a plot of CO_2 partial pressure versus CO oxidation rate (Figure 2). At comparable O_2 and CO_2 concentrations, i.e. in the 2-3 mol% CO_2 range, the inhibition effect of CO_2 can be approximated by a reaction order of about –0.57. With feed compositions of 3.5-4.0 mol% CO_2, however, the active surface is blocked progressively by CO_2, and eventually CO conversion is reduced to one-third of its initial level at 2 mol%. Although CO_2 adsorption on both Pt and CeO_x sites is possible, the decline observed

in CO conversions and CO oxidation rates appears to be caused by the effective blockage of oxygen transfer from the oxygen-bearing surface groups of AC2 to metal/metal oxide sites that facilitate oxygen reverse spillover from CeO_x to Pt sites. A similar negative effect of CO_2 is reported to operate on oxide-supported catalysts through obstruction of mobile oxygen and/or dissociation of CO_2 on metallic sites to increase the surface CO on Pt sites, leaving limited adsorption sites for oxygen.[21]

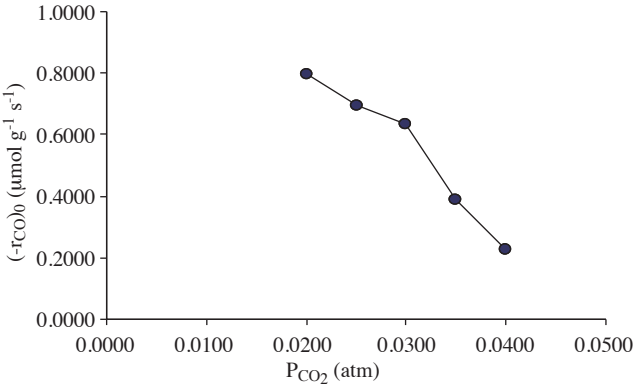

Figure 2. Effect of CO_2 on CO oxidation rates over 1wt%Pt-1wt%CeO_x/AC2 (T = 383 K; W/F_{CO} = 0.049 g s μmol^{-1}; λ = 1.0; TOS = 90 min).

The presence of H_2 under PROX conditions prevents the occurrence of similar inhibition by CO_2; in previous work on PROX over sequentially impregnated 1wt%Pt-1wt%CeO_x/AC2 at 423 K in feed containing 1 mol% CO, 1 mol% O_2 and 60 mol% H_2, CO conversion was found to increase drastically by partial replacement of inert diluent with 15 mol% CO_2.[12] It was suggested that the carbon atoms released on the AC2 support surface upon decomposition of surface groups could contribute to a spillover process by reversibly adsorbing CO_2, which may well eliminate its negative effect.

Effect of H_2 on CO oxidation

Previous work on selective CO oxidation in H_2-rich feed over 1wt%Pt-1wt%CeO_x/AC2 at 423 K conducted without and with CO_2 + H_2O in the feed gave 100% CO conversion for various feed compositions.[11,12] In the present study, the effect of the presence of H_2 on CO conversions and CO oxidation rates was examined under conditions used in the kinetic analysis, specifically in the initial rates region at 383 K, by partially replacing the inert He with 10-60 mol% H_2 in a feed with 5 mol% CO and 2.5 mol% O_2. The CO conversion levels and CO oxidation rates reached at a rather low space time W/F_{CO} = 0.049 g s μmol^{-1} with λ = 1.0 (stoichiometric) are presented in Table 3. These data show that CO conversion decreases with the introduction of H_2 into the feed but stays more or less in the same range above 20 mol% up to 60 mol% H_2.

In order to remove CO completely from H_2-rich gas in practice, O_2/CO ratios greater than 1.0 (i.e. $\lambda >$ 2) have to be employed; however, this also increases the likelihood of unwanted H_2 oxidation.[22] On the other hand, the use of stoichiometric proportions promotes the coverage of active Pt sites by CO, which decreases the adsorption probability of O_2 and limits both CO and H_2 oxidation, so that the 2 reactions are coupled, yielding a relatively constant selectivity level of about 40%.[17] In this work, the selectivity for CO oxidation

S_{CO}, defined as O_2 consumed in CO oxidation divided by total O_2 consumption, started off at 40% at lower hydrogen concentrations, decreased gradually to 30% with increasing H_2 partial pressure up to 20 mol% H_2 and then remained around 20-25% with some fluctuation. The loss of selectivity observed over Pt/γ-Al_2O_3 catalysts at low CO concentrations is explained by the commencement of CO desorption which also enhances H_2 oxidation.[16] Over Pt/CeO_2 catalysts, on the other hand, it is suggested that loss of selectivity is caused by the desorption of water, since oxygen-deficient CeO_2 stabilizes surface water, which reacts at the Pt-CeO_2 interface with adsorbed CO in a low-temperature water-gas shift reaction to produce CO_2.[8–10] Pt-based catalysts are also known to produce CO by reverse WGS at low space velocities as a result of O_2 depletion especially at extended reaction times and low O_2/CO ratios.[3]

The introduction of 10-60 mol% H_2 into the feed led to a gradual decrease in the CO oxidation rates over 1wt%Pt-1wt%CeO_x/AC2. In contrast, the H_2-induced enhancement in CO oxidation rates over 1wt%Pt-0.25wt%SnO_x/AC3 was nearly 10-fold at H_2 concentrations exceeding 30 mol% with a CO oxidation selectivity of about 46%.[15] Possible reasons for the improvement were suggested as the interaction of H_2 with oxygen-bearing surface groups of the AC3 support and/or with oxygen species adsorbed on Pt and Pt_3Sn alloy sites to diminish the oxidizing conditions provided by these species and to release some of the metallic sites for CO adsorption. Moreover, since the Pt_3Sn alloy has specific sites for both CO and O_2 adsorption, the need for oxygen transfer over the support surface is eliminated. In the same way, the explanations proposed for the 2-fold increase in CO oxidation rates over Pt/γ-Al_2O_3 included the interaction between the hydroxylated γ-Al_2O_3 support and CO adsorbed on Pt sites.[16] The present results on 1wt%Pt-1wt%CeO_x/AC2 appear to be along the line of reports on the role of surface water and the WGS effect in CO consumption, which may also provide a plausible explanation for the finding that, at 423 K, the addition of 15% CO_2 and 10% H_2O into a feed containing 1% CO, 1% O_2, and 60% H_2 by partially replacing the 38% inert He gives 100% CO conversion with 50% selectivity for CO oxidation.[12] If this is the case, the mechanisms of CO oxidation over CeO_2-containing Pt catalysts may be quite different in the absence and presence of H_2 and further work would be required to substantiate the behavior of AC2 supported Pt-CeO_x catalysts.

Conclusions

Kinetics of low temperature CO oxidation over 1wt%Pt-1wt%CeO_x/AC2 was studied at 383 K using a range of CO (1-5 mol %) and O_2 (1-2.5 mol %) concentrations corresponding to oxygen excess factors (λ) between 0.67 and 2.0. A power function rate expression with negative dependence on CO (–0.24) and positive dependence on O_2 (0.98) and a LHHW rate model are proposed for CO oxidation in the absence of H_2, indicating that the reaction takes place on a surface that is primarily covered by adsorbed CO with weak dissociative adsorption of oxygen as the rate-limiting step. Addition of 2-4 mol% CO_2 into a feed with 5 mol% CO and 2.5 mol% O_2 decreased the CO conversions and CO oxidation rates over sequentially impregnated 1wt%Pt-1wt%CeO_x/AC2, possibly by obstructing oxygen transfer to metal/metal oxide sites. Introduction of increasing amounts of H_2 between 10 and 60 mol% into the same feed led to loss of selectivity for CO oxidation, the reason for which may be the role of surface water and the WGS effect in CO consumption.

Acknowledgement

Financial support was provided by the TÜBİTAK project 104M163 and Boğaziçi University projects BAP-06HA501 and DPT-03K120250. The TÜBİTAK scholarship to B. Gülyüz and the TÜBA-GEBİP grant to A. E. Aksoylu are also acknowledged.

References

1. Trimm, D. L.; Önsan, Z. İ. *Catal. Rev. Sci. Eng.* **2001,** *43*, 31-84.
2. Trimm, D. L. *Appl. Catal. A Gen.* **2005,** *296*, 1-11.
3. Önsan, Z. İ. *Turk. J. Chem.* **2007,** *31*, 531-550.
4. Atalık, B.; Üner, D. *J. Catal.* **2006,** *241*, 268-275.
5. Gasteiger, H. A.; Kocha, S. S.; Sompalli, B.; Wagner, F. T. *Appl. Catal. B Environ.* **2005,** *56*, 9-35.
6. Oran, U.; Üner, D. *Appl. Catal. B. Environ.* **2004,** *54*, 183-191.
7. Wootsch, A.; Descorme, C.; Duprez, D. *J. Catal.* **2004,** 225, 259-266.
8. Pozdnyakova, O.; Teschner, D.; Wootsch, A.; Krohnert, J.; Steinhauer, B.; Sauer, H.; Toth, L.; Jentoft, F. C.; Knop-Gericke, A.; Paal, Z.; Schlögl, R. *J. Catal.* **2006,** *237*, 1-16.
9. Teschner, D.; Wootsch, A.; Pozdnyakova, O.; Sauer, H.; Knop-Gericke, A.; Schlögl, R. *React. Kinet. Catal. Lett.* **2006,** 87, *235*-247.
10. Pozdnyakova, O.; Teschner, D.; Wootsch, A.; Krohnert, J.; Steinhauer, B.; Sauer, H.; Toth, L.; Jentoft, F. C.; Knop-Gericke, A.; Paal, Z.; Schlögl, R. *J. Catal.* **2006,** *237*, 17-28.
11. Ş. Özkara, Ş; Aksoylu, A. E. *Appl. Catal. A Gen.* **2003,** *251*, 75-83.
12. Şimşek, E.; Özkara, Ş.; Aksoylu, A. E.; Önsan, Z. İ. *Appl. Catal. A: Gen.* **2007,** *316*, 169-174.
13. Aksoylu, A. E.; Freitas, M.M.A.; Figueiredo, J. L. *Appl. Catal. A: Gen.* **2000,** *192*, 29-42.
14. Aksoylu, A. E.; Freitas, M. M. A.; Pereira, M. F. R.; Figueiredo, J. L. *Carbon* **2001**, *39*, 175-185.
15. Soyal-Baltacıoğlu, F.; Gülyüz, B.; Aksoylu, A. E.; Önsan, Z. İ. *Turk. J. Chem.* **2007,** *31*, 455-464.
16. Kahlich, M. J.; Gasteiger, H. A.; Behm, R. J. *J. Catal.* **1997**, *171*, 93-105.
17. Schubert, M. M.; Kahlich, M. J.; Gasteiger, H. A.; Behm, R. J. *J. Power Sources* **1999,** *84*, 175-182.
18. Akın, A. N.; Kılaz, G.; İşli, A. İ.; Önsan, Z. İ. *Chem. Eng. Sci.* **2001,** *56*, 881-888.
19. Mieher, W. D.; Whitman, L. J.; Ho, W. *J. Chem. Phys.* **1989**, *91*, 3228-3239.
20. Pedersen, M. O.; Bocquet, M.-L.; Sautet, P.; Laegsgaard, E.; Stensgaard, I.; Besenbacher, F. *Chem. Phys. Lett.* **1999**, *299*, 403-409.
21. Manasilp, A.; Gulari, E. *Appl. Catal. B: Environ.* **2002,** *37*, 17-25.
22. Oh, S. H.; Sinkevitch, R. M. *J. Catal.* **1993**, *142*, 254-262.